CrossMark

ORIGINAL PAPER

Assessment of myocardial delayed enhancement with cardiac computed tomography in cardiomyopathies: a prospective comparison with delayed enhancement cardiac magnetic resonance imaging

Hye-Jeong Lee[1] · Dong Jin Im[1] · Jong-Chan Youn[2] · Suyon Chang[1] · Young Joo Suh[1] ·
Yoo Jin Hong[1] · Young Jin Kim[1] · Jin Hur[1] · Byoung Wook Choi[1]

Abstract To evaluate the feasibility of cardiac CT for the evaluation of myocardial delayed enhancement (MDE) in the assessment of patients with cardiomyopathy, compared to cardiac MRI. A total of 37 patients (mean age 54.9 ± 15.7 years, 24 men) who underwent cardiac MRI to evaluate cardiomyopathy were enrolled. Dual-energy ECG-gated cardiac CT was acquired 12 min after contrast injection. Two observers evaluated cardiac MRI and cardiac CT at different kV settings (100, 120 and 140 kV) independently for MDE pattern-classification (patchy, transmural, subendocardial, epicardial and mesocardial), differentiation between ischemic and non-ischemic cardiomyopathy and MDE quantification (percentage MDE). Kappa statics and the intraclass correlation coefficient were used for statistical analysis. Among different kV settings, 100-kV CT showed excellent agreements compared to cardiac MRI for MDE detection ($\kappa = 0.886$ and 0.873, respectively), MDE pattern-classification ($\kappa = 0.888$ and 0.881, respectively) and differentiation between ischemic and non-ischemic cardiomyopathy ($\kappa = 1.000$ and 0.893, respectively) for both Observer 1 and Observer 2. The Bland–Altman plot between MRI and 100-kV CT for the percentage MDE showed a very small bias (-0.15%) with 95% limits of agreement of -7.02 and 6.72. Cardiac CT using 100 kV might be an alternative method to cardiac MRI in the assessment of cardiomyopathy, particularly in patients with contraindications to cardiac MRI.

Keywords Cardiomyopathy · Myocardial delayed enhancement · Myocardial fibrosis · Cardiac computed tomography · Cardiac magnetic resonance imaging

Introduction

For cardiomyopathy, determining the exact etiology for each patient is important because etiology is directly related to treatment and patient survival [1]. In that sense, cardiac magnetic resonance imaging (MRI) with myocardial delayed enhancement (MDE) imaging using extracellular contrast agents has been well established for cardiomyopathy assessment [2, 3]. Typical patterns of MDE can classify ischemic cardiomyopathy from non-ischemic cardiomyopathy [4, 5] and MDE patterns can also help differentiate non-ischemic etiology [2]. MDE is not only used for diagnostic purposes, but also to collect information on the exact amount of irreversible myocardial damage, which helps predict patient prognosis in cardiomyopathy [6]. Although MRI with MDE imaging is now routine in clinical practice, contraindications for MRI, as well as its limited availability, have to be considered.

Iodinated contrast possesses contrast kinetics that parallel those of gadolinium. Therefore, in a method similar to that of cardiac MRI, the delayed enhancement technique can be performed by cardiac computed tomography (CT) [7, 8]. Delayed enhancement cardiac CT has actually shown its potential for visualizing myocardial infarction (MI) in earlier studies, but it was not valued as a clinical tool with single-slice CT [9]. However, recent studies have investigated the diagnostic value of cardiac CT in MI assessment

✉ Byoung Wook Choi
bchoi@yuhs.ac

1 Department of Radiology, Research Institute of Radiological Science, Severance Hospital, Yonsei University College of Medicine, 50-1 Yonsei-ro, Seodaemun-gu, Seoul 120-752, South Korea

2 Division of Cardiology, Cardiovascular Hospital, Severance Hospital, Yonsei University College of Medicine, 50-1 Yonsei-ro, Seodaemun-gu, Seoul 120-752, South Korea

with greatly improved spatial and temporal resolution of current multi-detector CT (MDCT) techniques [8, 10–13]. Consequently, we could hypothesize that cardiac CT may display the MDE of cardiomyopathy in a similar way to MRI. However, while delayed enhancement cardiac MRI for cardiomyopathy has been well established, there have been only a few clinical reports about the capacity of cardiac CT and even those have only covered hypertrophic cardiomyopathy (HCM) [14–16]. Therefore, the purpose of our study was to determine the feasibility of cardiac CT for MDE detection, pattern-classification, differentiation of ischemic and non-ischemic cardiomyopathy, and quantification in cardiomyopathy assessment. In addition, we evaluated whether a higher density of contrast enhancement in lower tube voltage (kV) was beneficial to the assessment of MDE in cardiomyopathy [17].

Methods

Study population

Our institutional ethics committee approved this prospective study. From June 2012 to March 2014, we identified 132 patients with suspected cardiomyopathy from clinical findings among patients who underwent cardiac MRI. Patients with other cardiac diseases such as congenital heart disease (six patients) and valvular heart disease (11 patients) were excluded. Eight patients were excluded due to cardiac function recovery on follow-up echocardiography. Nine patients were excluded due to poor general conditions that required treatment in the intensive care unit. Patients with iodine contrast allergy (three patients) or decreased renal function (seven patients) were also excluded. From 88 patients, 51 patients refused to participate in the study and a final total of 37 patients (24 men, 64.9%; mean age 54.86 ± 15.65 years, range 22–81 years) gave written informed consent and were enrolled in this study.

Cardiac MRI

Cardiac MRI was performed with a 3.0-T MRI imaging system (Magnetom Trio; Siemens Medical Solutions, Erlangen, Germany) and an eight-channel cardiac coil. Delayed enhancement imaging was performed 10 min after injection of gadobutrol (0.2 mmol/kg, Gadovist; Bayer Schering Pharma AG, Berlin, Germany) at 2 ml/s. Scanning parameters were as follows: segmented inversion recovery prepared turbo FLASH sequences, TR 9.9 ms, TE 4.9 ms, flip angle 20°, field of view 380×380 mm, matrix 320×320, slice thickness 8 mm with no gap in the short axis plane. Data acquisition was synchronized with ECG in

the mid-diastolic phase to minimize motion artifacts. After a variable trigger delay dependent on heart rate, a nonselective 180° pulse was applied. A variable inversion time (TI) determined by TI scout to null the signal intensity of the normal myocardium after contrast administration was used to allow longitudinal relaxation.

Cardiac CT

All CTs were performed with a second-generation dual source CT (Somatom Definition Flash; Siemens Medical Solutions, Forchheim, Germany) within 10 days of cardiac MRI. A bolus of Iopamidol (370 mg/ml of iodine, 1.8 ml/kg, Prosure 370, LG life science, Seoul, Korea) was injected into an antecubital vein at 3 ml/sec, followed by 40 ml of saline. 12 min after contrast injection, dual-energy CT was performed using the following parameters: retrospective ECG-gated acquisitions with tube current modulation (ECG-pulsing window 60–80%), 512×512 pixel matrix, 64×0.6 mm slice collimation, 162 mAs (effective) at 140 kV with tin (Sn) filter and 138 mAs (effective) at 100 kV, and 0.33 s rotation time. Scans were performed from the tracheal bifurcation to the diaphragm and the field of view was adjusted according to heart size.

From the raw data, images were automatically reconstructed into three image data sets: 100-kV, 140-kV and weighted averaged 120-kV images, which were fused images with 60% density information from the 100-kV image and 40% from the 140-kV image. The axial images were reconstructed at the mid-diastolic phase using a 0.75 mm slice thickness, a 0.5 mm increment interval, and a medium-smooth convolution kernel (D30f).

Image analysis

All CT and MRI images were reviewed on an offline workstation (AquarisNet Viewer V1.8.0.3, TeraRecon). MRI and CT were assessed by two radiologists (H.Y.J. and H.J with 6 and 9 years of experience in cardiac imaging, respectively) blinded to the results of the other imaging technique and the patients' clinical findings. CT images of each kV setting were reconstructed with short axis multiplanar images with 8 mm slice thickness and no gap for analysis. A narrow window width and level (approximately 200 and 100, respectively) were used to maximize the contrast between MDE and the normal myocardium. The diagnostic quality of CT images for MDE was classified as good (no artifacts, unrestricted evaluation), fair (minor to moderate artifacts, acceptable for evaluation), or poor (severe artifacts impairing accurate evaluation). Each observer reviewed the MRI, 100-kV CT, 120-kV CT and 140-kV CT images at 1-month intervals to reduce any learning effects.

For both MRI and CT, qualitative analyses using a 16-segment model of the left ventricle (LV) [18] were performed to assess MDE patterns. First, observers detected the presence of MDE for each segment with the normal myocardium defined as a region without any apparent high density/signal intensity at visual inspection. If MDE was observed, patterns were classified as patchy, transmural, subendocardial, epicardial, or mesocardial (Fig. 1). Then, observers classified cardiomyopathy as ischemic or non-ischemic with the location and pattern of MDE. Ischemic cardiomyopathy was defined as having MDE in the subendocardium or in a transmural location following a vascular territory. If not, non-ischemic cardiomyopathy was considered [3, 19, 20].

Quantitative analyses were also performed for MDE quantification on both MRI and CT. The endo- and epicardial contours of the LV were drawn manually in each section while excluding trabeculations and papillary muscles. The overall myocardial volume (LV volume) was calculated by subtracting the endocardial area from the epicardial area, with the difference being multiplied by section thickness. Afterwards, all hyperenhancing pixels on the MRI and CT images were manually traced and volume was calculated by multiplying the MDE area by section thickness (MDE volume). The percentage MDE was determined by dividing the MDE volume by the overall myocardial volume, with the quotient multiplied by 100.

Finally, the contrast-to-noise ratio (CNR) was acquired for each kV CT. Referring to cardiac MRI, observers drew the region of interest (ROI) in the center of the MDE and remote non-MDE myocardium at the mid LV in a consensus reading. The size and location of the ROI were kept constant for 100-kV, 120-kV and 140-kV CT using the copy and paste function. Mean values and standard deviations of Hounsfield units (HUs) were obtained from the ROI. Then, the CNR was calculated by dividing the difference in the mean HU between the MDE and remote non-MDE myocardium by the standard deviation of HU of the remote non-MDE myocardium.

Statistical analysis

Statistical analyses were performed with the SPSS software package (version 17.0 for Windows, SPSS Inc., Chicago, Illinois). For MDE detection, pattern-classification and differentiation between ischemic and non-ischemic cardiomyopathies, inter-observer and inter-test agreements were determined through kappa statistics using a contingency table. For the percentage MDE, inter-observer agreements were tested using the intraclass correlation coefficient

Fig. 1 Pattern-classification of myocardial delayed enhancement (MDE). The figure shows 100-kV CT images of (**a**) amyloidosis, (**b**) sarcoidosis, (**c**) DCM and (**d**) HCM. The subendocardial pattern (*arrow head*) was defined as MDE at the innermost myocardium, the epicardial pattern (*open arrow head*) was defined at the outermost myocardium, and the mesocardial pattern (*open arrow*) referred to MDE at the portion of the myocardium lying between the endocardium and epicardium. The transmural pattern (*asterisk*) was defined as having involvement from the endocardium to the epicardium. The patchy pattern (*arrows*) was regarded as nodular enhancement being observed anywhere on the myocardium. *MDE* myocardial delayed enhancement, *DCM* dilated cardiomyopathy, *HCM* hypertrophic cardiomyopathy
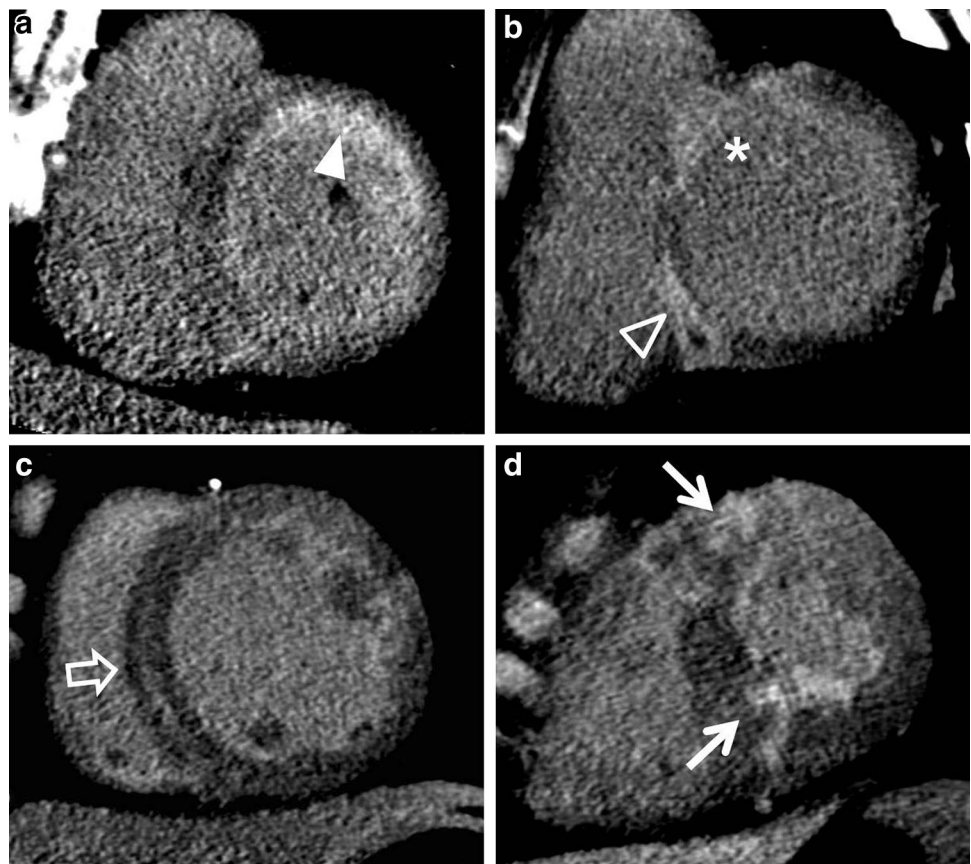
(ICC). Inter-test agreements were determined on the Bland–Altman plots and multiple observations (two observers) per subjects were considered [21]. Inter-observer agreements were found for MRI and each kV CT between the two observers. Inter-test agreements were found between MRI and each kV CT for each observer. The κ values and ICCs were interpreted as follows: 0.00–0.20, slight; 0.21–0.40, fair; 0.41–0.60, moderate; 0.61–0.80, good; and 0.81–1.00, excellent agreement [22]. The CNR of each kV CT was compared with the paired t test. A p value of <0.05 indicated a statistically significant difference.

Results

Baseline characteristics

There were five patients with ischemic cardiomyopathy and 32 patients with non-ischemic cardiomyopathy. Of non-ischemic cardiomyopathy, six patients had HCM, 13 dilated cardiomyopathy (DCM) (three alcoholic, two chemotherapy-related and eight idiopathic), five amyloidosis, five sarcoidosis and three chronic myocarditis. Ischemic cardiomyopathy, HCM and DCM were diagnosed from clinical findings with cardiac MRI findings. Chronic myocarditis was diagnosed from clinical history with or without a histopathological diagnosis. All patients with amyloidosis were confirmed with endomyocardial biopsy. Although patients with sarcoidosis were not diagnosed with endomyocardial biopsy, lung and lymph node biopsies showed sarcoidosis involvement.

The mean body mass index was 24.32 ± 3.58 kg/m^2 and ten patients were ≥ 25 kg/m^2. The mean effective radiation dose for CT was 6.81 ± 0.88 mSv. The mean injected contrast volume was 117.06 ± 25.68 ml. The mean heart rate for CT was 68.27 ± 12.47 bpm. All CT images showed good quality for MDE analysis except for seven patients with fair quality (18.9%, 7/37): the patients had artifacts at the anterior and/or anterolateral segment of the basal LV from chest wall structures, but the other segments were not affected by the artifacts. All myocardial segments were included for analysis.

MDE detection and pattern-classification

The results of inter-observer and inter-test agreements for MDE detection and pattern-classification are summarized in Table 1 and described in Fig. 2. For Observer 1, MRI showed MDE on 205 of 592 segments based on the 16-segment model. 100-kV CT and 120-kV CT showed excellent agreement with MRI (κ = 0.886 and 0.867, respectively) and 140-kV CT showed good agreement (κ = 0.699). For pattern-classification, patchy delayed enhancement was found in 29 segments, 39 transmural, 76 subendocardial, 41 epicardial, and 20 mesocardial on MRI. In addition, 100-kV CT and 120-kV CT showed excellent agreement with MRI (κ = 0.888 and 0.866, respectively) and 140-kV CT showed good agreement (κ = 0.699).

For Observer 2, MRI showed MDE on 214 of 592 segments, and 100-kV CT and 120-kV CT showed excellent agreement with MRI (κ = 0.873 and 0.869, respectively) and 140-kV CT showed good agreement (κ = 0.716). For pattern-classification, patchy delayed enhancement was found in 32 segments, 40 transmural, 76 subendocardial, 46 epicardial, and 20 mesocardial on MRI. 100-kV CT and 120-kV CT showed excellent agreement with MRI (κ = 0.881 and 0.872, respectively) and 140-kV CT showed good agreement (κ = 0.725).

Inter-observer agreements of MRI, 100-kV CT, 120-kV CT and 140-kV CT showed excellent agreement for the detection of MDE (κ = 0.952, 0.939, 0.938 and 0.930,

Table 1 The results of inter-test agreements for MDE detection and pattern-based classification

|	Observer 1				Observer 2			
	MRI	CT$_{100kV}$	CT$_{120kV}$	CT$_{140kV}$	MRI	CT$_{100kV}$	CT$_{120kV}$	CT$_{140kV}$
MDE segment	205	218	215	188	214	223	218	192
Kappa value[a]		0.886	0.867	0.699		0.873	0.869	0.716
MDE pattern								
Patchy	29	37	40	31	32	38	41	31
Transmural	39	41	39	44	40	41	41	49
Subendocardial	76	77	76	64	76	78	74	63
Epicardial	41	39	40	42	46	42	42	41
Mesocardial	20	24	20	7	20	24	20	8
Kappa value[a]		0.888	0.866	0.699		0.881	0.872	0.725

Values are segment numbers

MDE myocardial delayed enhancement

[a] Kappa value between MRI and each kV CT (inter-test agreement)

Fig. 2 Comparison of MRI and each kV CT in a patient with a clinical history of myocarditis. **a** MRI, **b** 100-kV CT, **c** 120-kV CT and **d** 140-kV CT. Mesocardial MDE at the anterior septum (*arrow*) and small patchy MDEs at the inferior septum (*arrow heads*) of the mid LV on MRI (**a**) is well delineated even on 100-kV CT (**b**). However, these MDEs are not definite on 120-kV CT (**c**). 140-kV CT (**d**) showed mesocardial MDE (*arrow*) on MRI (**a**) with an ill-defined patchy MDE (*open arrow*) and no small patchy MDEs. The transmural MDE at the inferior wall of the mid LV (*asterisk*) on MRI (**a**) is well delineated even on 100-kV (**b**) and 120-kV CT (**c**), but not on 140-kV CT (**d**). *MDE* myocardial delayed enhancement
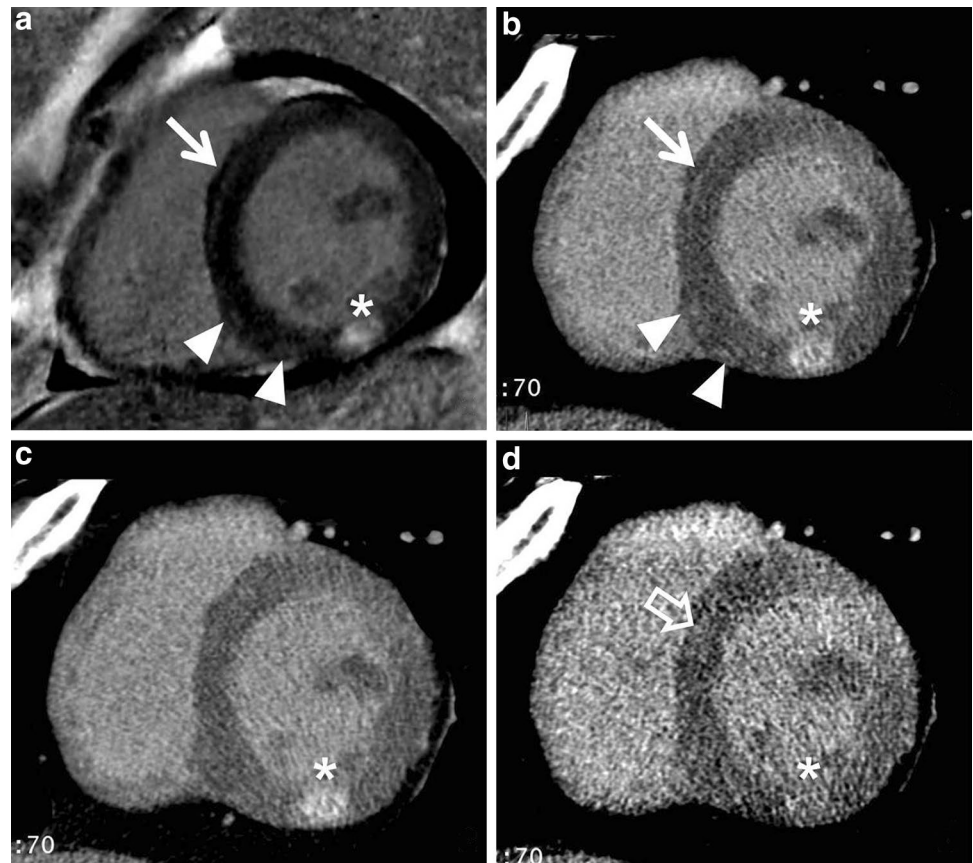
respectively) and pattern-classification ($\kappa = 0.942$, 0.926, 0.919 and 0.882, respectively).

Ischemic versus non-ischemic cardiomyopathy

At final diagnosis, there were five patients with ischemic cardiomyopathy and 32 patients with non-ischemic cardiomyopathy. Both Observer 1 and 2 concluded that five patients had ischemic cardiomyopathy and 32 patients had non-ischemic cardiomyopathy (inter-observer agreement, $\kappa = 1.000$) on cardiac MRI, and these results correlated with the final diagnoses. Results for differentiation between ischemic and non-ischemic cardiomyopathy are summarized in Table 2. Compared to cardiac MRI, Observer 1

noted excellent agreement with 100-kV CT ($\kappa = 1.000$) and good agreements with 120-kV and 140-kV CT ($\kappa = 0.893$ and 0.723, respectively). Observer 2 noted excellent agreements with 100-kV and 120-kV CT ($\kappa = 0.893$ for both) and good agreement with 140-kV CT ($\kappa = 0.654$). For inter-observer agreements, 100-kV and 120-kV CT showed excellent agreements ($\kappa = 0.893$ and 0.801, respectively), and 140-kV CT showed good agreement ($\kappa = 0.771$).

MDE quantification

For Observer 1, the percentage MDE was $16.70 \pm 15.42\%$, $17.19 \pm 15.03\%$, $17.12 \pm 14.78\%$ and $15.05 \pm 13.64\%$ on MRI, 100-kV, 120-kV and 140-kV CT, respectively. For

Table 2 The results of inter-observer and inter-test agreements for differential diagnosis between ischemic and non-ischemic cardiomyopathies

	Observer 1				Observer 2			
	MRI	CT_{100kV}	CT_{120kV}	CT_{140kV}	MRI	CT_{100kV}	CT_{120kV}	CT_{140kV}
Ischemic CM	5	5	6	8	5	6	6	9
Non-ischemic CM	32	32	31	29	30	31	31	28
Kappa value[a]		1.000	0.893	0.723		0.893	0.893	0.654

Values are patient numbers

CM cardiomyopathy

[a] Kappa value between MRI and each kV CT (inter-test agreement)

Observer 2, the percentage MDE was $16.85 \pm 15.90\%$, $16.65 \pm 15.11\%$, $16.98 \pm 14.75\%$ and $16.21 \pm 14.50\%$ on MRI, 100-kV, 120-kV and 140-kV CT, respectively. Inter-observer agreements of MRI, 100-kV CT, 120-kV CT and 140-kV CT were all excellent for the percentage MDE (ICC = 0.985, 0.986, 0.972 and 0.973, respectively). Bland–Altman plots between MRI and each kV CT are demonstrated in Fig. 3. For the 100-kV CT, a very small bias (−0.15%) with 95% limits of agreement of −7.02 and 6.72 was found. For the 120-kV CT, the agreement also showed a very small bias (−0.27%) and 95% limits of agreement from −7.71 to 7.15%. 140-kV CT showed a small bias of 1.14% with 95% limits of agreement from −11.36 to 13.64%.

CNR

Because delayed enhancement was not detected on MRI for six of 37 patients, CNR could not be calculated for these patients. For other 31 patients, the mean value of CNR was 3.70 ± 1.36 in 100-kV CT, 4.02 ± 1.25 in 120-kV CT and 1.70 ± 1.21 in 140-kV CT. For CNR, 120-kV CT showed a significantly higher CNR compared to 100-kV CT ($p = 0.006$) and 140-kV CT ($p < 0.001$).

Discussion

In this study, we evaluated the feasibility of cardiac CT for MDE detection, pattern-classification, differentiation of ischemic and non-ischemic cardiomyopathy, and quantification in cardiomyopathy assessment. The main finding of this study was that cardiac CT with tube voltages of 100 and 120 kV showed excellent agreements in assessing the MDE of cardiomyopathy compared to cardiac MRI. For MDE quantification, 100-kV and 120-kV CT showed small biases with more narrow ranges of 95% limits of agreement compared to 140-kV CT along with results comparable to prior studies [23].

Recently, more data have shown the feasibility of delayed enhancement cardiac CT for acute and chronic MI [8, 10–13]. It uses a premise similar to that for cardiac
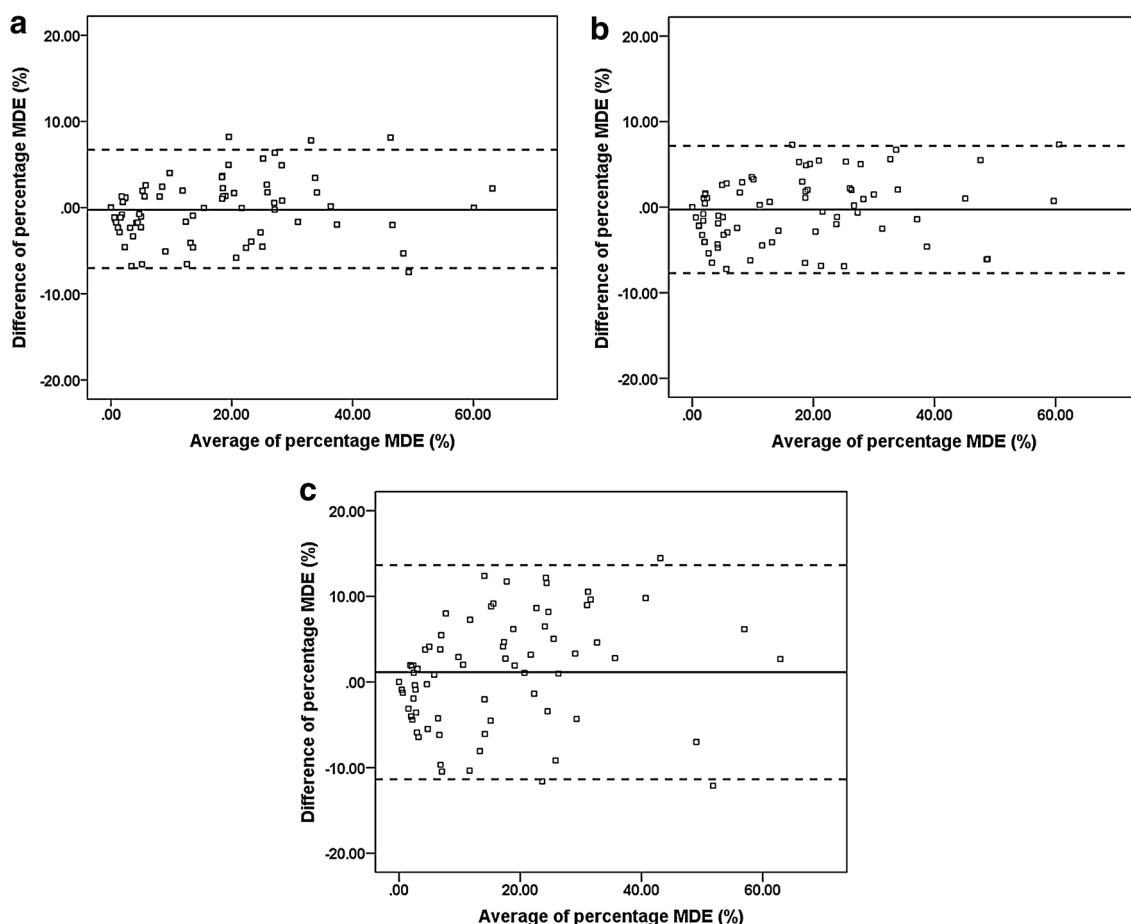
Fig. 3 Bland–Altman plots between MRI and each kV CT. **a** 100-kV CT, **b** 120-kV CT and **c** 140-kV CT. *Solid lines* represent mean difference (bias); *broken lines* represent 95% limits of agreement. *MDE* myocardial delayed enhancement

MRI, because the contrast agents used for cardiac CT and cardiac MRI are both primarily extracellular, interstitial agents with similar contrast kinetics [7, 8]. However, to our knowledge, only a few studies have focused on HCM among previous research on the CT evaluation of MDE in non-ischemic cardiomyopathy [14–16]. Although these studies showed that cardiac CT provides reliable detection and quantification of MDE in HCM, we thought that further study was needed as diverse patterns, extent and degrees of MDE can be shown in cardiomyopathies. As a result, cardiac CT might be a robust alternative method to cardiac MRI in the clinical assessment of cardiomyopathy on delayed enhancement imaging.

A major issue of cardiac CT that needs to be considered is radiation exposure. Furthermore, the low CNR can also be an issue because with cardiac CT, there are no means to null the normal myocardium and maximize the contrast difference with the abnormal myocardium in the evaluation of MDE. One way to solve these problems might be to reduce tube voltage [24, 25]. In this study, although 120-kV CT showed the highest CNR compared to CT of other kV settings, 100-kV CT also demonstrated excellent agreement compared to MRI and excellent inter-observer agreement for MDE assessment. The 80-kV setting was not evaluated as our scanner did not allow an 80-kV option in its dual-energy setting. Although previous research showed that the 80-kV setting was the lowest radiation dose option for MI [26], other CT studies showed that the 80-kV setting was unsuccessful in showing MDE. Therefore, a higher voltage setting was chosen in an attempt to minimize image noise [25] and 100 kV provided an acceptable CNR at a lower radiation dose compared to other kV settings. However, although we did include 10 patients (27.0%, 10/37) with BMI ≥ 25 kg/m^2 in this study, further studies with 100 kV for these patients might be necessary.

The contrast injection protocol could be an issue for delayed enhancement cardiac CT, with contrast volume being especially problematic. There is currently no consensus on the optimal protocol. Generally, MDE is detected in patients who receive more contrast ($\geq$1.5 ml/kg) in myocardial infarction. We used a contrast volume of 117 ml with 370 mg/ml of iodine. Prior studies for HCM used a wide range of contrast volume from 80 to 90 ml (370 mg/ml of iodine) to 150 ml (370 mg/ml or 350 mg/ml of iodine) [14–16]. In addition, the prior studies with HCM showed comparable results with a shorter time interval of 7 min between contrast injection and image acquisition for delayed enhancement cardiac CT [14–16]. Further studies are needed to determine the optimal minimum contrast volume and time interval for delayed enhancement cardiac CT in cardiomyopathies. We performed manual quantification for MDE in the present study because there is currently no consensus for

semi-automated MDE quantification and no available commercial software for MDE quantification with cardiac CT. Although manual quantification is a widely used method in daily clinical practice, future development of a semi-automated quantitative technique based on the pixel intensity map is expected to result in more accurate MDE quantification with cardiac CT.

In this study, seven patients showed fair quality images due to artifacts from the adjacent chest wall structures. These artifacts could have particularly disrupted evaluation of the anterior or anterolateral segment of the basal LV. We thought that these artifacts were discernible because they showed a lower high-density compared to usual MDE and were in line with the outside of the heart on successive images. However, ultimately, artifacts from the chest wall should be resolved to further establish delayed enhancement cardiac CT as a reliable and accurate method.

This study has some limitations. First, this preliminary study involved a small number of patients. Although the 16-segment model had a satisfactory number of MDE patterns collected for analysis, a larger population study might be necessary for further validation. Second, this study included some patients with relatively high frequency of MDE segments. This might affect kappa statics for inter-test and inter-observer agreements, especially for MDE detection. Third, right ventricular MDE was not evaluated in this study because cardiomyopathies with right ventricular MDE on cardiac MRI are relatively rare. Further studies are needed to assess the value of delayed enhancement cardiac CT in the evaluation of right ventricular MDE. Fourth, in this study the mean effective radiation dose for CT was 6.81 mSv. This value might have resulted because we performed dual-energy CT with retrospective ECG-gating scanning as our scanner did not allow prospective ECG-gating with the dual-energy setting. However, the single-energy setting with prospective ECG-gated image acquisition promises to reduce radiation exposure even more [27].

In conclusion, cardiac CT might be a robust alternative method to cardiac MRI in the assessment of cardiomyopathy, particularly in patients with contraindications to cardiac MRI. The 100-kV setting might help to reduce radiation exposure and provide acceptable CNR for delayed enhancement cardiac CT. High spatial resolution, short scan times, and the accessibility of CT scanners are the main advantages of MDCT. It would also be desirable to establish a comprehensive CT examination which provides information about coronary artery disease, myocardial morphology, and MDE in cardiomyopathy patients in the future. However, imaging parameters must be further optimized and the CNR further improved with artifacts being resolved before MDCT can be recommended as an everyday clinical tool for cardiomyopathy assessment.

References

1. Felker GM, Thompson RE, Hare JM et al (2000) Underlying causes and long-term survival in patients with initially unexplained cardiomyopathy. N Engl J Med 342(15):1077–1084
2. Mahrholdt H, Wagner A, Judd RM, Sechtem U, Kim RJ (2005) Delayed enhancement cardiovascular magnetic resonance assessment of non-ischaemic cardiomyopathies. Eur Heart J 26(15):1461–1474
3. Cummings KW, Bhalla S, Javidan-Nejad C, Bierhals AJ, Gutierrez FR, Woodard PK (2009) A pattern-based approach to assessment of delayed enhancement in nonischemic cardiomyopathy at MR imaging. Radiographics 29(1):89–103
4. Wu E, Judd RM, Vargas JD, Klocke FJ, Bonow RO, Kim RJ (2001) Visualisation of presence, location, and transmural extent of healed Q-wave and non-Q-wave myocardial infarction. Lancet 357(9249):21–28
5. McCrohon JA, Moon JC, Prasad SK et al (2003) Differentiation of heart failure related to dilated cardiomyopathy and coronary artery disease using gadolinium-enhanced cardiovascular magnetic resonance. Circulation 108(1):54–59
6. Aljaroudi WA, Flamm SD, Saliba W, Wilkoff BL, Kwon D (2013) Role of CMR imaging in risk stratification for sudden cardiac death. JACC Cardiovasc Imaging 6(3):392–406
7. Allard M, Doucet D, Kien P, Bonnemain B, Caille JM (1988) Experimental study of A-gadolinium. Pharmacokinetics and pharmacologic properties. Invest Radiol 23(Suppl 1):S271–S274
8. Gerber BL, Belge B, Legros GJ et al (2006) Characterization of acute and chronic myocardial infarcts by multidetector computed tomography: comparison with contrast-enhanced magnetic resonance. Circulation 113(6):823–833
9. Gray WR, Buja LM, Hagler HK, Parkey RW, Willerson JT (1978) Computed tomography for localization and sizing of experimental acute myocardial infarcts. Circulation 58(3 Pt 1):497–504
10. Mahnken AH, Koos R, Katoh M et al (2005) Assessment of myocardial viability in reperfused acute myocardial infarction using 16-slice computed tomography in comparison to magnetic resonance imaging. J Am Coll Cardiol 45(12):2042–2047
11. Lardo AC, Cordeiro MA, Silva C et al (2006) Contrast-enhanced multidetector computed tomography viability imaging after myocardial infarction: characterization of myocyte death, microvascular obstruction, and chronic scar. Circulation 113(3):394–404
12. Wichmann JL, Bauer RW, Doss M et al (2013) Diagnostic accuracy of late iodine-enhancement dual-energy computed tomography for the detection of chronic myocardial infarction compared with late gadolinium-enhancement 3-T magnetic resonance imaging. Invest Radiol 48(12):851–856
13. Wichmann JL, Arbaciauskaite R, Kerl JM et al (2014) Evaluation of monoenergetic late iodine enhancement dual-energy computed tomography for imaging of chronic myocardial infarction. Eur Radiol 24(6):1211–1218
14. Shiozaki AA, Senra T, Arteaga E et al (2013) Myocardial fibrosis detected by cardiac CT predicts ventricular fibrillation/ventricular tachycardia events in patients with hypertrophic cardiomyopathy. J Cardiovasc Comput Tomogr 7(3):173–181
15. Zhao L, Ma X, Delano MC et al (2013) Assessment of myocardial fibrosis and coronary arteries in hypertrophic cardiomyopathy using combined arterial and delayed enhanced CT: comparison with MR and coronary angiography. Eur Radiol 23(4):1034–1043
16. Langer C, Lutz M, Eden M et al (2014) Hypertrophic cardiomyopathy in cardiac CT: a validation study on the detection of intramyocardial fibrosis in consecutive patients. Int J Cardiovasc Imaging 30(3):659–667
17. Nakayama Y, Awai K, Funama Y et al (2005) Abdominal CT with low tube voltage: preliminary observations about radiation dose, contrast enhancement, image quality, and noise. Radiology 237(3):945–951
18. Cerqueira MD, Weissman NJ, Dilsizian V et al (2002) Standardized myocardial segmentation and nomenclature for tomographic imaging of the heart. A statement for healthcare professionals from the Cardiac Imaging Committee of the Council on Clinical Cardiology of the American Heart Association. Circulation 105(4):539–542
19. Richardson P, McKenna W, Bristow M et al (1996) Report of the 1995 World Health Organization/International Society and Federation of Cardiology Task Force on the Definition and Classification of cardiomyopathies. Circulation 93(5):841–842
20. Bluemke DA (2010) MRI of nonischemic cardiomyopathy. Am J Roentgenol 195(4):935–940
21. Bland JM, Altman DG (2007) Agreement between methods of measurement with multiple observations per individual. J Biopharm Stat 17(4):571–582
22. Landis JR, Koch GG (1977) The measurement of observer agreement for categorical data. Biometrics 33(1):159–174
23. Zhao L, Ma X, Feuchtner GM, Zhang C, Fan Z (2014) Quantification of myocardial delayed enhancement and wall thickness in hypertrophic cardiomyopathy: multidetector computed tomography versus magnetic resonance imaging. Eur J Radiol 83(10):1778–1785
24. Mendoza DD, Weigold WG (2009) Evaluation of myocardial viability by multidetector CT. J Cardiovasc Comput Tomogr 3(1 Suppl):S2–S12
25. Mendoza DD, Joshi SB, Weissman G, Taylor AJ, Weigold WG (2010) Viability imaging by cardiac computed tomography. J Cardiovasc Comput Tomogr 4(2):83–91
26. Mahnken AH, Bruners P, Muhlenbruch G et al (2007) Low tube voltage improves computed tomography imaging of delayed myocardial contrast enhancement in an experimental acute myocardial infarction model. Invest Radiol 42(2):123–129
27. Chang HJ, George RT, Schuleri KH et al (2009) Prospective electrocardiogram-gated delayed enhanced multidetector computed tomography accurately quantifies infarct size and reduces radiation exposure. JACC Cardiovasc Imaging 2(4):412–420